Strength and Deformation Characteristics of Reconstituted Sand under Different Stress Paths in True Triaxial Tests

Hasbullah Nawir[1,*], Bagus Eko Prasetyo[2] & Andhika Sahadewa[1]

[1]Geotechnical Engineering Research Group, Faculty of Civil and Environmental Engineering, Institut Teknologi Bandung, Jalan Ganesha No.10, Bandung 40132, Indonesia
[2]Civil Engineering Department, Sembilanbelas November University, Jalan Pemuda No. 399 Kolaka, South East Sulawesi, Indonesia
E-mail: hasbullah@si.itb.ac.id

Highlights:

- The true triaxial test has been developed to alleviate the limitations of the conventional Triaxial compression and triaxial extension test.
- The effect of intermediate stress on the true triaxial test causes an increase in the value of the friction angle until a certain value.
- The use of different stress paths in true triaxial test resulted in different soil parameter values, including modulus elasticity, E50.

Abstract. To improve the geotechnical stress–strain analysis, the stress–strain behavior of geomaterial under general three-dimensional stress conditions prevailing in the field need to be captured. The true triaxial apparatus is an enhanced version of the conventional triaxial apparatus, which allows to simulate stresses by applying loadings independently in 3 orthogonal directions. This study evaluated the strength and deformation behavior of Bangka sand under true triaxial test conditions. The test specimens were prepared by means of the multi-sieve sand pluviation method. Various true triaxial test stress paths were applied under axial compression, lateral extension, axial extension, and lateral compression with the objective of understanding and developing the empirical correlation of coarse-grained soil strength parameters in axial compression stress paths related to other stress paths. The test results showed that an increase in the value of b, the parameter used to quantify the relative magnitude of the intermediate principal stress to the other principal stresses, resulted in an increase of the internal friction angle and a decrease of the peak stress ratio. In addition it was observed that the Lade-Duncan failure criterion fitted the results of this study better than other failure criteria, namely the extended von Mises, Mohr-Coulomb, and Matsuoka-Nakai failure criteria.

Keywords: *axial compression; axial extension; failure criteria; intermediate principal stress; lateral compression; lateral extension; reconstituted sand; stress path*.

Received January 14th, 2020, 1st Revision July 15th, 2020, 2nd Revision August 26th, 2020, Accepted for publication September 17th, 2020.
 ISSN: 2337-5779, DOI: 10.5614/j.eng.technol.sci.2020.52.6.10

1 Introduction

To study the strength and deformation characteristics of various soils, typically, the conventional triaxial test is conducted by applying deviatoric stresses in the axial direction to a solid cylindrical soil specimen that was previously consolidated/unconsolidated under isotropic stress conditions. In the triaxial compression (TC) test, which is the most popular conventional triaxial test method, the axial stress is equal to the major principal stress (σ_1), which is increased at a controlled rate in axial compression (AC) mode. To replicate a uniform axisymmetric stress condition in the TC test, the intermediate (σ_2) and the minor (σ_3) principal stresses are set to the same magnitude to serve as confining pressure (σ_{radial}), which is normally kept constant during testing. The TC test is usually used to evaluate soil parameters for a variety of geotechnical analyses. Using the same triaxial apparatus for conducting TC, a triaxial extension (TE) test can also be performed. In the TE test, the σ_1 direction is horizontal while σ_2 is equal to σ_3. However, the actual stress conditions in the field can be more complex than those of the TC or the TE. In this case, the direction of σ_1 may be different from the vertical or horizontal directions, while σ_2 may not be equal to σ_3 nor to σ_1. This study aimed to contribute to a deeper understanding that can be used as a basis if complex conditions occur that cannot be simplified.

The true (or cubical) triaxial test has been developed to alleviate the limitations of the conventional TC and TE tests. In contrast to a conventional triaxial cell, a true triaxial cell (TTC) has a cubical frame with six faces, enabling a cubical soil specimen to be tested under different stress conditions resulted from independent loadings in 3 orthogonal stress directions. The early development of TTC was presented by Ko & Scott [1]. Subsequently, this stress-controlled TTC was further developed by Sture [2], Farias & Azevedo [3], Reddy, *et al.* [4], and Reis, *et al.* [5]. Meanwhile, strain-controlled TTC (Prashant & Penumadu [6]) and partially stress–strain controlled TTC (Green [7]; Lade [8]) have also been developed. Sture [2] suggests that the stress-controlled TTC appears to have more advantages in stress state control. Recently, stress-suction controlled TTC has been developed to test saturated and unsaturated soils (Matsuoka, *et al.* [9]; Hoyos & Macari [10]; Hoyos, *et al.* [11]; and Reis, *et al.* [5]). In the last few decades, the true triaxial test was employed by several researchers to study the mechanical behavior of various soil types, for example, to explore the stress–strain behavior of clays in the principal stress space (e.g. Wood [12]; Prashant & Penumadu [6]; Yin & Kumruzzaman [13]); to study the strength and deformation

characteristics of clays (e.g. Nakai, *et al*. [14]; Callisto & Calabresi [15]; Anantanasakul & Kaliakin [16]; Ye *et al*. [17]); to study shear banding and failure characteristics of sands (e.g. Wang & Lade [18]); and to study anisotropic deformation characteristics of sands (e.g. Yamada & Ishihara [19]; Lade, *et al.* [20]).

Despite all of these extensive studies, only a limited amount of true triaxial tests have been performed to study the behavior of Indonesian soils. Furthermore, only limited studies have been conducted to evaluate differences in soil parameters, whether obtained by an increase or a decrease of the mean principal stress. In the present study, the mean principal stress increase was evaluated using axial compression (AC) and lateral compression (LC) tests, whereas the mean principal stress decrease was studied using axial extension (AE) and lateral extension (LE) tests.

In the present study, the effects of inherent (or structural) anisotropy on the strength and deformation characteristics of sand were considered. Inherent anisotropy is attributed to fabric orientation controlled by the deposition of particles in the vertical direction. In laboratory stress–strain tests, the effects of anisotropic soil fabric orientation on the stress–strain behavior can be evaluated by loading at various σ_1 directions relative to the bedding plane, as reported in Lam & Tatsuoka [21]. They prepared cross-anisotropic sand specimens at a various deposition directions relative to the σ_1, σ_2, and σ_3 directions. This deposition direction is defined by two angles, ω and ξ, as shown in Figure 1. The variation of the deposition direction is currently being studied using the TTC apparatus used in this study. This manuscript presents only the deposition directions ω = X and $\xi = Y$.

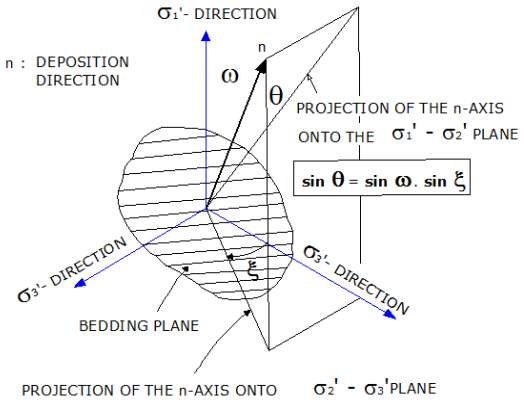

Figure 1 Definition of deposition direction with respect to the direction of the principal stress axes (after Lam & Tatsuoka [21].

This paper presents the results from an experimental study on the strength and deformation parameters of reconstituted natural Bangka sand loaded along different stress paths in true triaxial tests using an apparatus developed at Institut Teknologi Bandung (ITB), as descibed by Marlando [22]. The cubical specimens were prepared by the multi-sieve sand pluviation (MSP) method. A series of stress controlled true triaxial tests was performed to evaluate the stress and strain characteristics of reconstituted specimens of natural Bangka sand, in particular the effects of intermediate principal stress and changes in the mean principal stress during loading on soil parameters. Discussions on the effects of the intermediate stress ratio parameter (b) on E50 are limited. The results of this study provide new information on this issue, although more study is needed to capture the general picture in this respect. In addition, this study also aimed to validate the obtained soil parameters for incorporation into a widely employed soil constitutive model used in numerical analysis.

2 Test Procedure

2.1 Test Sand and Specimen Preparation

Bangka sand, the sample source in this study, is dominantly composed of quartz, which is considered representative of many natural sand materials in Indonesia. The specific gravity of the Bangka sand particles was 2.67. The grain size distribution curves of the Bangka sand specimens and those from other studies are shown in Figure 2. In this study, the tested sand was obtained by sieving to a range of 0.1 mm to 1.0 mm. The complete result of the physical testing is shown in Table 1.

Table 1 Physical properties of sand used in this study.

Material Properties	Value
d_{10} *(mm)*	0.15
d_{30} *(mm)*	0.22
d_{60} *(mm)*	0.35
Coefficient of uniformity (Cu)	2.33
Coefficient of curvature (Cc)	0.92
Minimum void ratio	0.709
Maximum void ratio	0.851
Minimum dry density (g/cm^3)	1.44
Maximum dry density (g/cm^3)	1.59

A set of 80-mm cubical specimens with controlled densities was carefully prepared by means of a reproducible and reliable method, called the multi-sieve sand pluviation method (Miura & Toki [23]). The particle fall height from the last sieve to the base of the specimen mould was 300 mm, with a particle flow rate of 0.54 cm^3/s. The prepared specimens had relative densities ranging from 80% to 90% (dense to very dense). Inherent anisotropy has significant effects on the strength and deformation characteristics of soil (Lam & Tatsuoka [21]; Hong & Lade [24]; Lade & Kirkgard [25]). In this study, all specimens were prepared using fixed deposition directions $\omega = 0°$ and $\xi = 90°$ (see Figure 1). At the time of writing, the effects of cross-anisotropy on the strength and deformation characteristics of reconstituted Bangka sand were still under study.

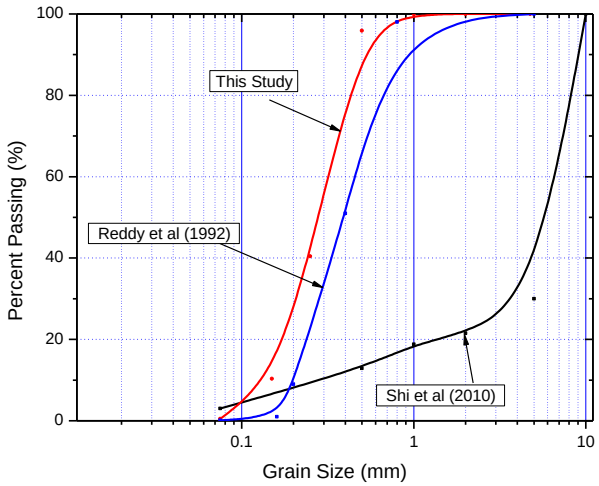

Figure 2 Grain size distribution curves of the samples compared with the grain size distribution from previous studies.

2.2 True Triaxial Apparatus

The stress-controlled true triaxial apparatus developed at Bandung Institute of Technology (ITB) is shown in Figure 3. The main components of this apparatus are a cubical TTC, a stress control system, a measurement system, and a data acquisition system. The cubical TTC comprises a solid aluminum cubical frame (Figure 4) to support the wall assemblies (Figure 5) and the soil specimen. Six connection bolts are provided on each face of the frame to attach and fix the wall assemblies. To transmit the applied pressure uniformly to the specimen, 1-mm thick low stiffness membranes are attached on the faces of the specimen. The membranes were prepared in the laboratory using silicone rubber with a maximum tear strength capacity of 510 kN/m^2 (74 psi). Information regarding this true triaxial apparatus is presented in more detail by Marlando [22].

Figure 3 True triaxial cell apparatus developed at ITB.

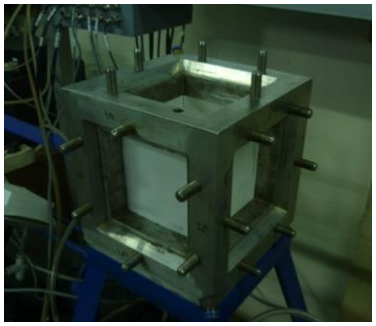

Figure 4 Cubical true triaxial frame.

Figure 5 Wall assemblies and the attached LVDT.

The stress control system developed in this study comprises an air compressor, tube pressure gauges, valves, and manually operated pressure regulators. Using a set of 3 pressure regulators (i.e. in the x, y, and z axis), application of different stresses on the 3 principal stress directions of the specimen is allowed. Thus, any specific stress paths can be set. The pressure is measured using transducers with a maximum capacity of 414 kN/m^2 (60 psi).

The deformation of the specimen is measured at a point on each of its six faces using 6 LVDTs. Volume changes of the specimen are determined using the specimen dimensions measured using the LVDTs. Two data acquisition devices are used in this system, (1) for the pressure transducers and (2) for the 6 LVDTs, respectively. Each data acquisition system comprises a signal conditioner and an analog-to-digital converter (A/D converter). Subsequently, the digital signals are transmitted to a computer. Data acquisition is performed using a special computer program.

2.3 Test Program

A series of true triaxial tests were conducted on in total 30 specimens under consolidated drained condition (CD) in order to evaluate the effects of intermediate principal stress on soil parameters under different stress paths. First, the specimens were saturated and consolidated under isotropic confining pressure (i.e. $\sigma_1 = \sigma_2 = \sigma_3$). Subsequently, a selected specific stress path was applied to the specimen by manually controlling the 3 independent pressure regulators of the stress control system. The stress paths imposed on the specimens in this study comprised: (i) axial compression (AC); (ii) lateral compression (LC); (iii) axial extension (AE); and (iv) lateral extension (LE). The tests were also conducted on octahedral planes with various intermediate stress ratio values, defined as

$$b = \frac{\sigma_2 - \sigma_3}{\sigma_1 - \sigma_3} \tag{1}$$

where σ_1, σ_2, and σ_3 are the major, the intermediate, and the minor principal stress, respectively. Since σ_3 was kept constant,

$$\Delta\sigma_2 = b\Delta\sigma_1 \tag{2}$$

where $\Delta\sigma_1$ and $\Delta\sigma_2$ are the increment of the major and the intermediate principal stress, respectively. In this study, the b parameter was varied at 0, 0.2, 0.4, 0.6, 0.8, and 1.0. The same method was used by Zhang *et al.* [26] to determine the value of b.

The axis convention is shown in Figure 6. The subscripts x and z refer to the horizontal directions and y refers to the vertical direction. It is assumed that there is no friction on the faces of the specimen. Thus, the normal stresses (σ_x, σ_y, σ_z) and normal strains (ε_x, ε_y, ε_z) on the side faces of the specimen are the principal components of the stress and strain tensors. The specimens were loaded under stress control corresponding to a stress increment rate of 3.45 kPa/min (0.5 psi/min). Loading and unloading cycles were performed in each test.

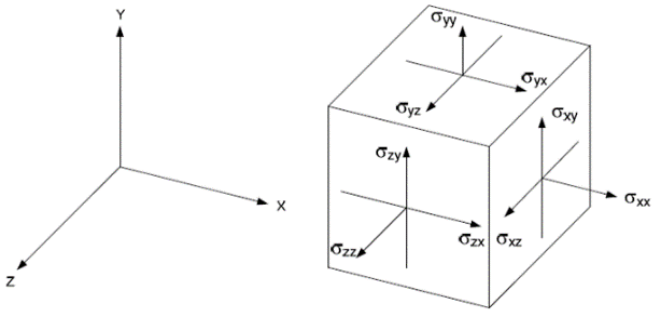

Figure 6 Axis convention in the true triaxial test.

The testing program conducted in this study is summarized in Table 2. The first 12 specimens were tested to evaluate the stress–strain behavior at b values of 0.0 and 1.0. In the AC and LC tests, confining pressures (σ_3) of 34.47 kN/m^2 (5 psi), 51.71 kN/m^2 (7.5 psi), and 68.95 kN/m^2 (10 psi) were applied. In AE and LE tests, confining pressures (σ), of 206.84 kN / m^2 (30 psi), 275.79 kN/m^2 (40 psi), and 344.74 kN/m^2 (50 psi) were applied.

Table 2 Specimens and testing program.

Physical Properties of Specimens			**Testing Program**					
e_o	γ_d (g/cm^3)	D_r (%)	**b**	**Stress Path**	**Octahedral Region**	**Loading Scheme**	**Confining Pressure (σ_c) (psi)**	**(kPa)**
0.732	1.51	83.44				$\Delta\sigma_{xx}$=0	5.00	34.47
0.728	1.51	86.31	0	AC (loading)	*A*	$\Delta\sigma_{yy}\neq$0 (+)	7.50	51.71
0.726	1.52	87.74				$\Delta\sigma_{zz}$=0	10.00	68.95
0.724	1.52	89.17				$\Delta\sigma_{xx}\neq$0 (+)	5.00	34.47
0.728	1.51	86.31		LC (loading)	*D*	$\Delta\sigma_{yy}$=0	7.50	51.71
0.726	1.52	87.74				$\Delta\sigma_{zz}\neq$0 (+)	10.00	68.95
0.732	1.51	83.44	1			$\Delta\sigma_{xx}$=0	30.00	206.84
0.722	1.52	90.59		AE (unloading)	*D*	$\Delta\sigma_{yy}\neq$0 (-)	40.00	275.79
0.732	1.51	83.44				$\Delta\sigma_{zz}$=0	50.00	344.74
0.728	1.51	86.31				$\Delta\sigma_{xx}\neq$0 (-)	30.00	206.84
0.722	1.52	90.59	0	LE (unloading)	*A*	$\Delta\sigma_{yy}$=0	40.00	275.79
0.724	1.52	89.17				$\Delta\sigma_{zz}\neq$0 (-)	50.00	344.74
0.73	1.51	84.87				$\Delta\sigma_{xx}$ = 0	2.50	17.24
0.722	1.52	90.59		AC (loading)	*A - B*	$\Delta\sigma_{yy}\neq$0 (+)	3.70	25.51
0.726	1.51	87.74				$\Delta\sigma_{zz}\neq$0 (+)	5.00	34.47
0.718	1.52	93.43				$\Delta\sigma_{xx}$=0	30.00	206.84
0.718	1.52	93.43	0.2	AE (unloading)	*C-D*	$\Delta\sigma_{yy}\neq$0 (-)	40.00	275.79
0.73	1.51	84.87				$\Delta\sigma_{zz}\neq$0 (-)	50.00	344.74
0.732	1.51	83.44				$\Delta\sigma_{xx}\neq$0 (-)	30.00	206.84
0.722	1.52	90.59		LE (unloading)	*A - B*	$\Delta\sigma_{yy}$=0	40.00	275.79
0.73	1.51	84.87				$\Delta\sigma_{zz}\neq$0 (-)	50.00	344.74
0.734	1.51	81.99				$\Delta\sigma_{xx}$=0,	2.50	17.24
0.726	1.52	87.74	0.6	AC (loading)	*A - B*	$\Delta\sigma_{yy}\neq$0 (+)	3.70	25.51
0.738	1.51	79.10				$\Delta\sigma_{zz}\neq$0 (+)	5.00	34.47
0.726	1.52	87.60				$\Delta\sigma_{xx}$=0,	2.50	17.24
0.724	1.52	89.01	0.4	AC (loading)	*A - B*	$\Delta\sigma_{yy}\neq$0 (+)	3.70	25.51
0.732	1.51	83.30				$\Delta\sigma_{zz}\neq$0 (+)	5.00	34.47
0.731	1.52	84.73				$\Delta\sigma_{xx}$=0,	2.50	17.24
0.724	1.52	89.01	0.8	AC (loading)	*A - B*	$\Delta\sigma_{yy}\neq$0 (+)	3.70	25.51
0.722	1.52	90.40				$\Delta\sigma_{zz}\neq$0 (+)	5.00	34.47

The deviatoric stress (q) was increased with a stress rate of 3.45 kPa/min (0.5 psi/min). Another set of 18 specimens were tested to evaluate the stress-

deformation behavior at b values > 1.0. In the AC tests, confining pressures (σ_3) of 17.24 kN/m^2 (2.5 psi), 25.51 kN/m^2 (3.7 psi), and 34.47 kN/m^2 (5 psi) were applied. In the AE and LE tests, the confining pressures (σ_1) were the same as for the first 12 specimens. All the results will be presented in the octahedral plane plot, as shown in Figure 7.

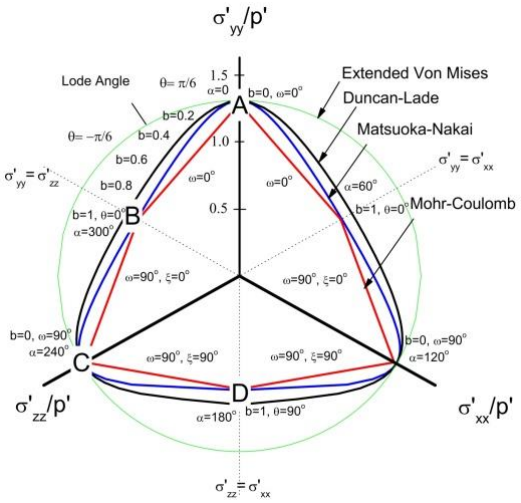

Figure 7 Position of octahedral plane plot.

3 Test Results

3.1 Tests at b = 0.0 and 1.0

The results of the triaxial tests at b = 0 (i.e. $\sigma_2 = \sigma_3$) or b = 1.0 (i.e. $\sigma_2 = \sigma_1$) are presented in Figure 8. In these figures, q and the mean effective principal stress (p) are respectively defined as:

$$q = \frac{1}{\sqrt{2}}[(\sigma_1 - \sigma_2)^2 + (\sigma_2 - \sigma_3)^2 + (\sigma_3 - \sigma_1)^2]^{1/2} \quad (3)$$

$$p' = \frac{1}{3}(\sigma_1' + \sigma_2' + \sigma_3') \quad (4)$$

In the AC test, sample-1, sample-2, and sample-3 were tested successively at $\sigma_2 = \sigma_3$ = 34.47 kN/m^2 (5 psi), 51.71 kN/m^2 (7.5 psi), and 68.95 kN/m^2 (10 psi) by increasing the deviatoric stress $\sigma_1 - \sigma_3$ ($+\Delta\sigma_{yy}$) at 345 kPa/min (0.5 psi/min) while keeping $\sigma_2 = \sigma_3$ ($\sigma_{xx} = \sigma_{zz}$) constant. In the LC test, sample-4, sample-5, and sample-6 were successively tested at σ_3 = 34.47 kN/m^2 (5 psi), 51.71 kN/m^2 (7.5 psi), and 68.95 kN/m^2 (10 psi) by increasing the deviatoric stress $\sigma_1 - \sigma_3$ ($\Delta\sigma_{xx} = \Delta\sigma_{zz}$) at 345 kPa/min (0.5 psi/min) while keeping σ_3 (σ_{yy}) constant.

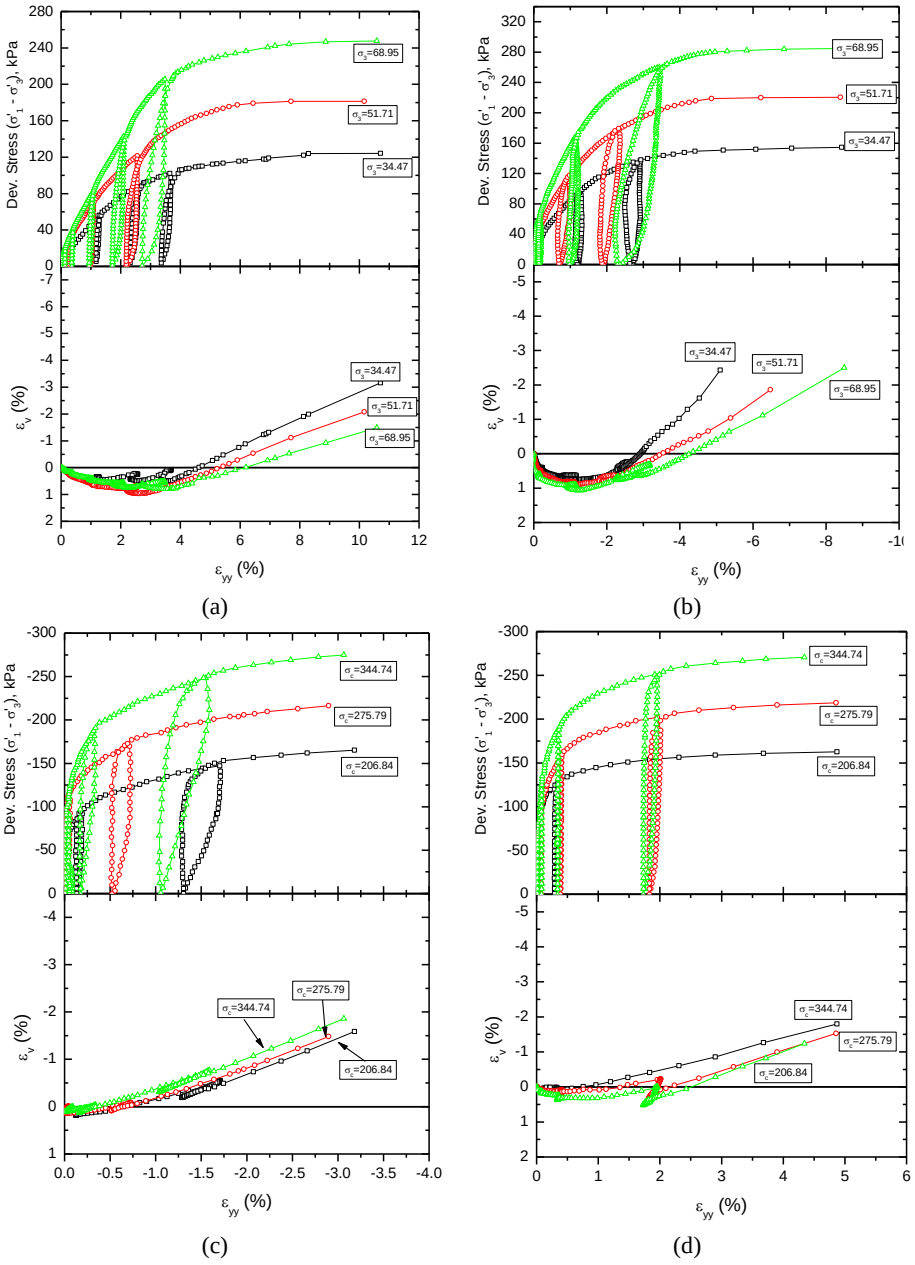

Figure 8 Stress-strain-volumetric curve of (a) AC true triaxial test at b = 0,:(b) LC at b = 1, (c) AE at b =1, and (d) LE at b = 0.

In the AE tests, sample-7, sample-8, and sample-9 were successively tested at $\sigma_1 = \sigma_2 = 206.84$ kN/m^2 (30 psi), 275.79 kN/m^2 (40 psi), and 344.74 kN/m^2 (50 psi) by increasing the deviatoric stress $\sigma_1 - \sigma_3$ ($-\Delta\sigma_{yy}$) at 345 kPa/min (0.5 psi/min) while keeping $\sigma_1 = \sigma_2$ ($\sigma_{xx} = \sigma_{zz}$) constant. In the LE test, sample-10, sample-11, and sample-12 were successively tested at $\sigma_1 = 206.84$ kN/m^2 (30 psi), 275.79 kN/m^2 (40 psi), and 344.74 kN/m^2 (50 psi) by increasing the deviatoric stress $\sigma_1 - \sigma_3$ ($-\Delta\sigma_{xx} = -\Delta\sigma_{zz}$) at 345 kPa/min (0.5 psi/min) while keeping σ_1 (σ_{yy}) constant.

3.2 Tests at b= 0.2, 0.4, 0.6 and 0.8

The results of the triaxial tests with influence from the intermediate principal stress (i.e. $\sigma 2 \neq \sigma 3$), where b = 0.2, 0.4, 0.6 and 0.8 are tabulated in Table 6. The effect of the intermediate stress on the values of the mechanical parameters and the elastic modulus of the sample is evaluated below.

4 Discussion

4.1 Strength Parameters

In the true triaxial test, b = 0 implies that $\sigma_2 = \sigma_3$ in the AC tests and LE tests, while b = 1.0 implies that $\sigma_2 = \sigma_1$ in the AE tests and LC tests. The angle of internal friction ϕ is influenced by the value of b. Figure 9 shows the values of ϕ plotted against b. The results from the failure criteria proposed by Lade & Duncan [27] are also shown in this figure. From this figure, it appears that ϕ increases with b. However, at b larger than 0.8, ϕ seems to decrease with b. This trend is in general the same as the predicted failure criteria in Shi *et al.* [28], Yin & Kumruzzaman [13] and Lade & Duncan [27]. Zhang *et al*. [26] got a value of ϕ that tended to rise following the increase of b up to 0.75.

Reddy, *et al.* [4] produced ϕ values that tended to be constant. Lam & Tatsuoka [21] conducted comprehensive studies on the effects of the initial anisotropic fabric and σ_2 on the strength and deformation characteristics of Toyoura sand. In their studies, sand specimens were prepared with a variety of deposition directions (i.e. ω and ξ) as well as compression and extension testing programs. The testing result using deposition directions $\omega = 0°$ and $\xi = 90°$ in compression is presented in Figure 9.

It can be seen that for b ranging from 0.2 to 0.8, the result from Lam & Tatsuoka [21] agrees well with the result from this study. It is observed that $M_f = q/p'$, where the definitions of q and p' are given by Eqs. (3) and (4), decreases as b increases (Figure 10). These results are also confirmed by previous research results.

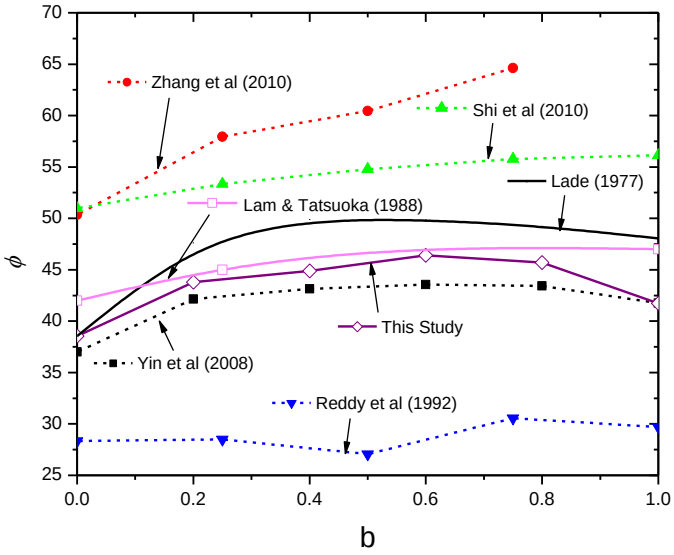

Figure 9 The effect of the value of b on the shear angle (ϕ).

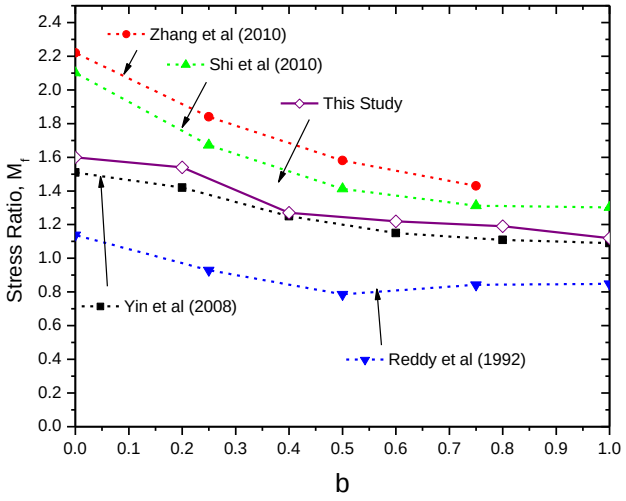

Figure 10 The effect of the value of b on the stress ratio (M_f).

4.2 Failure Surface on Octahedral Stress Plane (pi Plane)

The octahedral normal stress (σ'_{oct}) and the octahedral shear stress (τ'_{oct}) are shown in the following equations:

$$\sigma'_{oct} = \frac{1}{3}(\sigma'_1 + \sigma'_2 + \sigma'_3) \quad (5)$$

$$\tau'_{oct} = \frac{1}{3}[(\sigma'_1 - \sigma'_2)^2 + (\sigma'_2 - \sigma'_3)^2 + (\sigma'_3 - \sigma'_1)^2]^{1/2} \quad (6)$$

In the π plane, the true triaxial data at the time of failure are plotted as normalized principal stress to mean stress. The failure surface was compared against several failure criteria, namely the Mohr-Coulomb, extended von Mises (σ_{VM2} = 3J2), Duncan Lade ($k = I_{13} / I_3$), and Matsuoka-Nakai ($k = I_1 I_2 / I_3$) failure criteria. The angle value of Lode (θ) for the value of b (0-0.5) is π / 6 (30°) and b (0.5-1) -π / 6 (-30°). The octahedral shear stress data are shown in Figure 11. The failure criteria from this study fitted the Duncan-Lade failure criteria better than the other failure criteria.

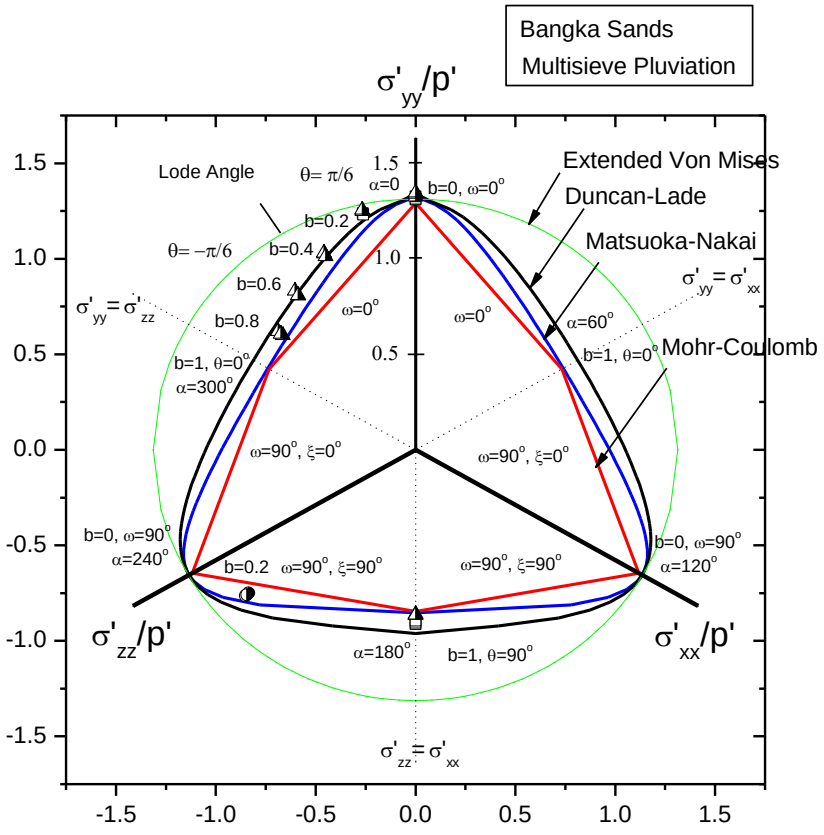

Figure 11 Normalized failure surface in an octahedral plane.

4.3 Shear Modulus

The modulus degradation is usually shown by the relationship between the normalized shear modulus (G/G_O) and the shear strain (γ). The G_O (G_{max}) is the maximum shear modulus value at small strain in elastic condition. The relationship between G_O, Young's modulus (E_O), and Poisson's ratio (ν) is pictured in the Figure 12.

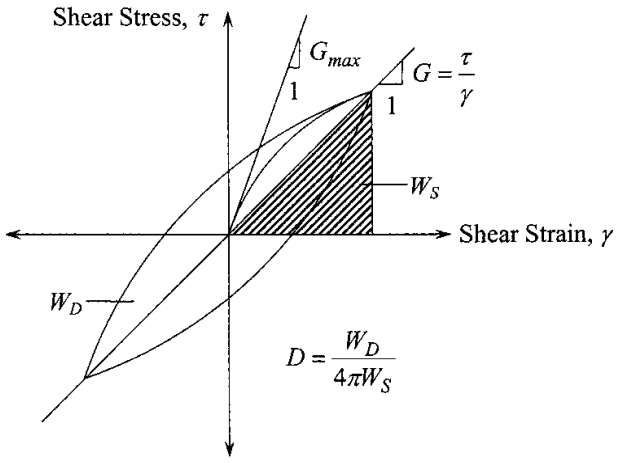

Figure 12 Shear modulus in the τ-γ field (Zhang *et al.* [26]).

In a true triaxial test that uses stress control, small strains are very difficult to observe. This G_O value is usually obtained from a resonant column test. Hardin [29] introduced the correlation of G_{max} or G_O values for effective confining pressure (σ_c') and the void ratio value (e) for soils with clean sand types, as shown in the following equation:

$$G_o = \frac{625}{(0.3+0.7e^2)} P_a{}^{0.5} \sigma_c{}^{0.5} \tag{7}$$

where Pa is the atmospheric pressure. Hardin & Drnevich [30] introduced the non-linear relationship of soil under small to medium strain using the hyperbolic stress–strain relationship in the following equation:

$$\frac{G}{G_o} = \frac{1}{1+\left(\frac{\gamma}{\gamma_r}\right)} \tag{8}$$

where γ_r is the reference shear strain value. According to Oztoprak & Bolton [31], the value of γ_r is the reference strain value in G/GO = 0.5. The value of γ from a

true triaxial test can be obtained from the deviatoric strain formulation in a 3D field using the Cambridge method as shown in the following equation:

$$\gamma, \varepsilon_d = \frac{\sqrt{2}}{3}\sqrt{(\varepsilon_x - \varepsilon_y)^2 + (\varepsilon_y - \varepsilon_z)^2 + (\varepsilon_z - \varepsilon_x)^2} \quad (9)$$

The shear modulus degradation is influenced by the confining pressure.

Figure 13 shows the degradation curves under different confining pressures, namely 34.47 kPa, 51.71 kPa and 68.95 kPa. The γ_{ref} values under these confining pressures calculated using Hardin & Drnevich's [30] hyperbolic models are shown in this figure. Thus, we can obtain the maximum and minimum range values of γ_{ref} from shear modulus degradation for all stress path mechanisms tested in this study (Table 3 and Figure 14).

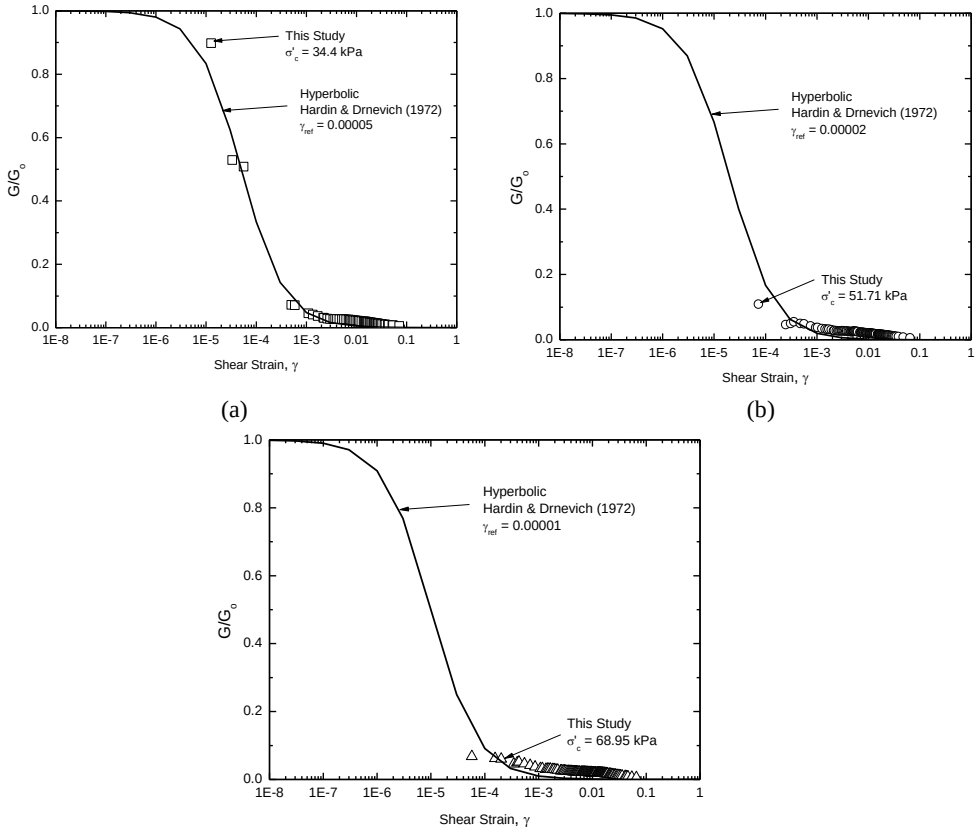

Figure 13 Shear modulus degradation behavior plot of the true triaxial data for the axial compression (AC) mechanism b = 0, (a) σ'c = 34.4 kPa, (b) σ'c = 51.71 kPa, (c) σ'c = 68.95 kPa.

Table 3 Maximum Go and γr values from the true triaxial test results

	Go	**γ_r**
Max	3299799	1.20E-04
Min	161540.7	1.02E-06
Mean	1476931	1.11E-05

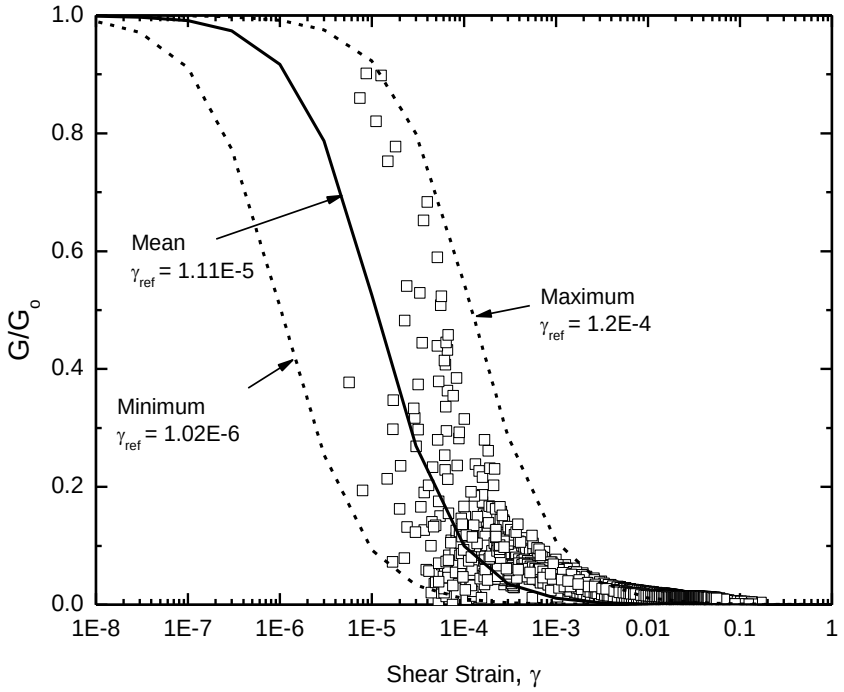

Figure 14 Plot of the shear modulus degradation behavior of the data from the true triaxial of Bangka sand for all stress path mechanisms and curve fittings and methods in Hardin & Drnevich [30].

The empirical correlations proposed by Hardin [29] to determine the G_O values are based on the resonant column, the cyclic triaxial test, and the triaxial compression test. Thus, theoretically, the correlation is closely related to the compression mechanism. If G/G_O and γ_{ref} in the true triaxial data are plotted on a logarithmic scale, the result is an unequal linear relationship between the compression and extension mechanisms. Eventually, this leads to an empirical correlation combination of compression and extension mechanisms, as shown in Figure 15.

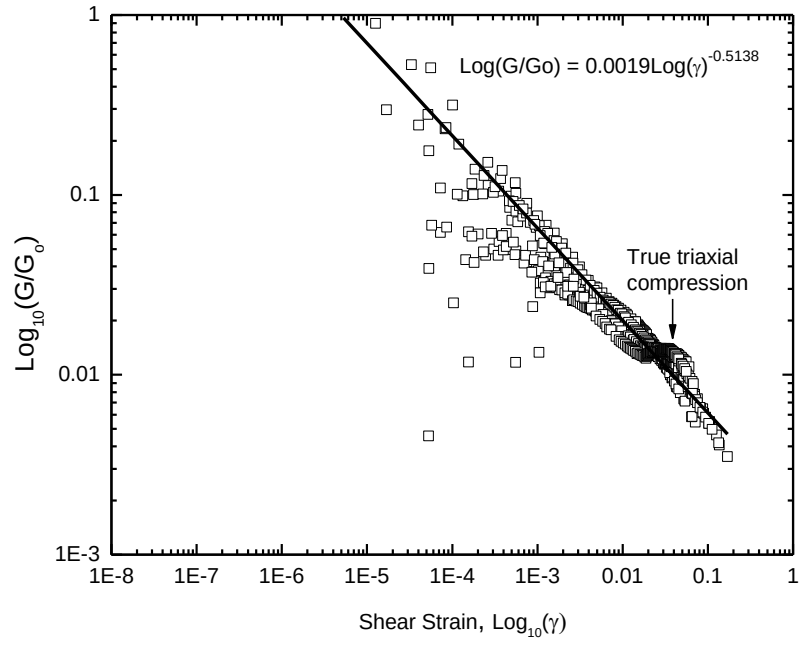

(a)

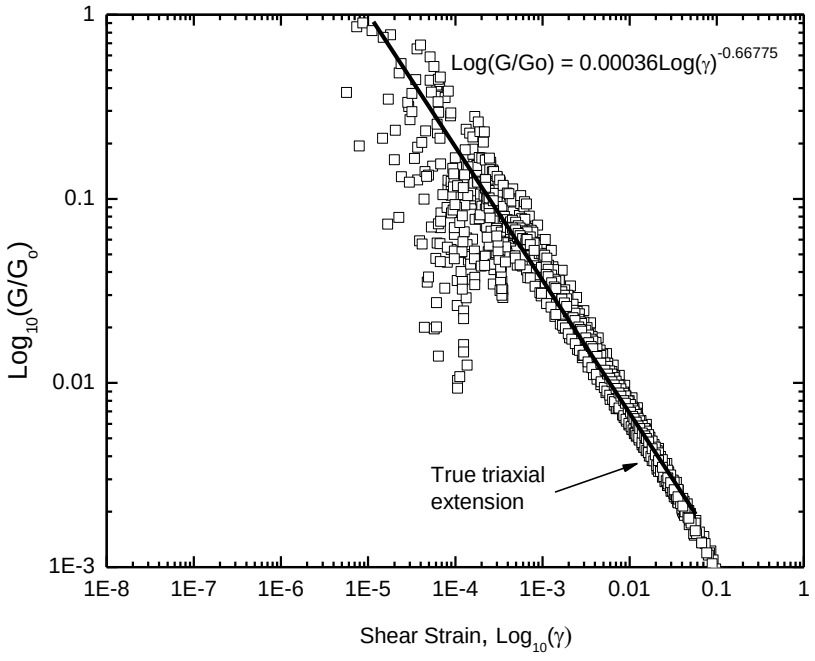

(b)

Figure 15 Empirical correlation log (G/GO) versus log (γ) of Bangka sand for a) the compression mechanism, and b) the extension mechanism

The empirical relationship for the triaxial compression mechanism is shown in the following equation:

$$\text{Log}(G/G_O) = 0.0583\text{Log}(\gamma) - 0.23434 \quad (10)$$

$$\text{Log}(G/G_O) = 0.0019\text{Log}(\gamma) - 0.5138 \quad (11)$$

The following equation shows the relationship for the extension mechanism:

$$\text{Log}(G/G_O) = 0.00036\text{Log}(\gamma) - 0.66775 \quad (12)$$

4.4 Secant Modulus

From this study, the comparison of the secant modulus (E_{50}) with the previous studies conducted by Yin & Kumruzzaman [13] and Shi, *et al.* [28] show similarities, even though the E_{50} comparison value produced by Yin & Kumruzzaman [13] was slightly larger, as shown in Table 4. The lowest value of E_{50} was obtained in the AC stress path, as shown in Table 5. The table also shows the results from the previous study conducted by Ng [32] and Wang [33].

Table 4 Comparison of secant modulus parameter (E50) against the value of b with compression loading mechanism.

Researchers	Secant Modulus Parameter (E_{50})
Yin & Kumruzzaman. [13]	$E_{50(b=0.2)} = 1.99\ E_{50(b=0)}$ $E_{50(b=1)} = 1.35\ E_{50(b=0)}$
Shi, *et al*. [28]	$E_{50(b=0.25)} = 1.16\ E_{50(b=0)}$ $E_{50(b=1)} = 1.45\ E_{50(b=0)}$
This study	$E_{50(b=0.2)} = 1.2\ E_{50(b=0)}$ $E_{50(b=1)} = 1.67\ E_{50(b=0)}$

Table 5 Comparison of secant modulus parameter (E_{50}) to stress path without intermediate stress (σ_2).

	This Study	Ng [32]	Wang [33]
AC	1.00	1.00	1.00
LE	4.37	2.14	-
AE	4.84	1.89	1.96
LC	1.67	1.03	-

In this study, the strength and deformation parameters from different stress paths were obtained as summarized in Table 6. The application of these parameters in suitable cases in the field will be evaluated in a future study.

Table 6 Summary of soil parameters obtained from the true triaxial tests.

Test Program		Strength Parameters				Deformation Parameters							
b	Stress Path	(kPa)	c' (kPa)	ϕ' (o)	M_f	E_i (kPa)	E_{50} (kPa)	E_{ur} average (kPa)	E_{ur} per Cycle (kPa) 1	2	3	4	5
0	AC	34.47	0.91	38.56	1.6	14706	5500	45263	53500	51200	42222	33933	
		51.71	0.91	38.56	1.61	15882	7000	45790	49240	45288	42639		
		68.95	0.91	38.56	1.62	16471	8800	46842	58300	54200	48222	39933	33000
1	LC	34.47	2.4	41.73	1.12	12000	10000	55000	88000	45000	32000		
		51.71	2.4	41.73	1.11	24000	12000	64000	89000	69000	34000		
		68.95	2.4	41.73	1.09	28000	15000	65000	92000	75000	28000		
1	AE	206.84	1.64	39.3	1.06	42000	25400	55000	75000	45290	44710		
		275.79	1.64	39.3	1.06	47500	34300	59000	78000	54790	44210		
		344.74	1.64	39.3	1.05	53000	43400	65000	85000	63000	47000		
0	LE	206.84	1.25	39.62	1.65	47600	20500	147000	147000	147000	147000	147000	
		275.79	1.25	39.62	1.64	55000	31500	135099	138099	135099	135099	132000	
		344.74	1.25	39.62	1.62	76000	41000	144300	150300	144300	144300	138500	
0.2	AC	17.24	2.99	43.8	1.55	10000	3500	26500	32000	25500	22000		
		25.51	2.99	43.8	1.54	13600	4300	29000	35000	27000	25000		

5 Conclusion

The test results indicate that the stress–strain behavior of unbound geomaterial is not exclusively determined by the two-dimensional stress condition on the plane along which the maximum stress obliquity is controlled by σ_1 and σ_3 only; the intermediate principal stress σ_2 also contributes to the stress–strain behavior. On the other hand, in ordinary engineering practice, only triaxial compression tests (with b = 0 and the direction of σ_1 normal to the bedding plane, e.g. in point A in Figure 7) are performed, while tests at other stress states, particularly those at b larger than 0.0 up to 1.0, are rarely performed. The conclusions listed below will contribute to the construction of a relevant stress–strain model under three-dimensional stress conditions from the results from the triaxial compression tests.

1. Sand sample preparation using the multi-sieve pluviation method can produce samples with a relatively good uniformity level of void ratio and relative density. This method is capable of producing samples with void ratio between 0.718 and 0.738 with a standard deviation of 0.00489. This method also results in a more even distribution of sand particles thus allowing evaluation of strength and deformation characteristics of reconstituted sand using relatively similar specimens.
2. The effect of intermediate stress (σ_2) on the true triaxial test causes an increase in the value of the friction angle (ϕ) until reaching b = 0.6. After b = 0.6, ϕ tends to decrease.
3. The octahedral plane shows that the failure criteria of Bangka sand in this study in general fit the failure criteria of Duncan-Lade better than other failure criteria.
4. The stress ratio M_f decreased as b increased.
5. The relationship between G/Go and γ is linear and varies depending on the compression/extension mechanism used to generate the data.
6. The use of different stress paths in the true triaxial test resulted in different soil parameter values, including E_{50}. In testing without considering the effect of the intermediate stress (σ_2) on soil parameters, the smallest and the greatest E_{50} values were generated by the AC stress path and AE stress path, respectively.
7. Comparison of the value of unloading-reloading modulus (Eur) with the secant modulus (E_{50}) in the true triaxial test without the effect of σ_2 yielded a varying ratio. In this test it is known that the value of Eur generated from the application of different confining pressures does not change significantly, where the value of E_{50} will be greater if the confining pressure given is also

greater. Thus, the ratio between Eur and E_{50} will be smaller if the confining pressure used is greater.

References

[1] Ko, H.Y. & Scott, R.F., *A New Soil Testing Apparatus*, Geotechnique, **17**(1), pp. 40-57, 1967.

[2] Sture, S., *Development of Multiaxial Cubical Test Device with Porewater Pressure Monitoring Facilities*, Report No. VPI-E-79.18, Dept. Civil Eng., Virginia Poly. Inst. & State U., Blacksburg, VA, 1979. (Technical Report).

[3] Farias, M.M. & Azevedo, R.F., *Cubical Triaxial Test in Dry Sand*, Proceeding of the VIII Brazilian Congress of Soil Mechanics and Foundation Engineering (CBMSEF), Porto Alegre, Vol. 2, Brazilian Association of Soil Mechanics and Geotechnical Engineering, Sao Paulo, Brazil, pp. 33-44, August 1986.

[4] Reddy, K.R., Saxena, S.K. & Budiman, J.S., *Development of a True Triaxial Testing Apparatus*, Geotechnical Testing Journal, **15**(2), pp. 89-105, 1992.

[5] Reis, R.M., Azevedo, R.F., Botelho, B.S. & Vilar, O.M., *Performance of a Cubical Triaxial Apparatus for Testing Saturated and Unsaturated Soils*, Geotechnical Testing Journal, **34**(3), pp. 177-185, 2011.

[6] Prashant, A. & Penumadu, D., *Effect of Intermediate Principal Stress on Overconsolidated Kaolin Clay*, J. Geotech. Geoenviron. Eng., ASCE, **3**(284), pp. 284-292, 2014.

[7] Green, C.S., *Strength and Deformation of a Sand Measured in an Independent Stress Control Cell*. Proceeding of The Roscoe Memorial Symposium on Stress Strain Behavior of Soils, Cambridge, UK, March 29-31, R.H.G. Parry, Ed., G.T., Foulisand Co. Ltd., Henley-on-Thames, UK, pp. 285-323, 1971.

[8] Lade, P.V., *The Stress Strain and Strength Characteristics of Cohesionless Soils*, PhD Thesis, University of California, Berkeley, Berkeley CA, 1972.

[9] Matsuoka, D.A., Sun, D.A., Ando, M., Kogane, A. & Fukuzawa, N., *Deformation and Strength of Unsaturated Soil by True Triaxial Test*, Proc. of Second International Conf. on Unsaturated Soils, Vol. 1, Beijing, China, International Academic Publisher, pp. 410-415, August 1998.

[10] Hoyos, L.R., Jr. & Macari, E.J., *Development of a Stress/Suction-Controlled True Triaxial Testing Device for Unsaturated Soils*, Geotech Test J., **24**(1), pp. 5-13, 2001.

[11] Hoyos, L.R., Laikram, A. & Puppala, A.J., *A Novel True Triaxial Apparatus for Testing Unsaturated Soils Under Suction-Controlled Multi-Axial Stress States*, Proc. 16th Int. Conf. of Soil Mechanics and

Geotechnical Eng., Osaka, Japan, Sept. 12-16, ISSMGE, London, pp. 387-390, 2015.

[12] Wood, D.M., *Explorations of Principal Stress Space with Kaolin in a True Triaxial Apparatus*, Geotechnique, **25**(4), pp. 783-797, 1975.

[13] Yin, H.J. & Kumruzzaman, Md., *The Stress-Strain-Strenght Behaviour of a Completely Decomposed Granite Soil Using a New Advanced True Triaxial Testing System*, International Association for Computer Methods and Advances in Geomechanics, IACMAG, pp. 1571-1579, 2008.

[14] Nakai, T., Matsuoka, H., Okuno, N. & Tsuzuki, K., *True Triaxial Tests on Normally Consolidated Clay and Analysis of the Observed Shear Behavior Using Elastoplastic Constitutive Models*, Soils and Foundations, **26**(4), pp. 67-78, 1986.

[15] Callisto, L. & Calabresi, G., *Mechanical Behaviour of a Natural Soft Clay*, Geotechnique, **48**(4), pp. 495-513, 1998.

[16] Anantanasakul, P. & Kaliakin, V.N., *Simulations Of 3-D Drained Behavior of Normally Consolidated Clay Using Elastoplastic Models*, In R. Hryciw, A. Athanasopoulos-Zekkos N. Yesiller (Eds.), GeoCongress 2012, pp. 1076-1085, 2012.

[17] Ye, G.L., Sheng, J.R. & Wang, J.H., *Automated True Triaxial Apparatus and its Application to Over-consolidated Clay*, Geotechnical Testing Journal, **35**(4), pp. 1-12, 2012.

[18] Wang, Q. & Lade, P.V., *Shear Banding in True Triaxial Tests and Its Effect on Failure in Sand*, J. Eng. Mech., **127**(8), pp. 754-761, 2001.

[19] Yamada, Y. & Ishihara, K., *Anisotropic Deformation Characteristics of Sand Under Three-Dimensional Stress Conditions*, Soils and Foundations, **19**(2), pp. 79-94, 1979.

[20] Lade, P.V., Rodriguez, N.M. & Van Dyck, E.J., *Effect of Principal Stress Directioon 3D Failure Condition in Cross-Anisotropic Sand*, Journal of Geotechnical and Geoenvironmental Eng., **140**(2), pp. 362-363, 2013.

[21] Lam, W. K. & Tatsuoka, F., *Effects of Initial Anisotropic Fabric and σ2 on Strength and Deformation Characteristics of Sand*, Soils and Foundations, **28**(1), pp. 89-106, 1988.

[22] Marlando, E.M.L., *Development of True Triaxial Cell and Its Use in the Behavior Study of Stress and Strain Response of Tropical Clay Soil in Bandung*, Master Thesis, Faculty of Civil and Environmental Engineering, Institut Teknologi Bandung, 2013. (Text in Indonesian)

[23] Miura, S. & Toki, S., *A Sample Preparation Methodand its Effect on Static and Cyclic Deformation Strength Properties of Sand*, Soils and Foundations, **22**(1), pp. 61-77, 1982.

[24] Hong, W.P. & Lade, P.V., *Elasto-plastic Behavior of K0-consolidated Clay in Torsion Shear Tests*, Soils and Foundations, **29**(2), pp. 127-140, 1989.
[25] Lade, P.V. & Kirkgard, M.M., *Effects of Stress Rotation and Changes of b-values on Cross-anisotropic Behavior of Natural K0-consolidated Soft Clay*, Soils and Foundations, **40**(6), pp. 93-105, 2000.
[26] Zhang, Y., Zhu, J. & Zhang, K., *True Triaxial Experiments of Coarse-grained Soils*, Proceeding of the 20th International Offshore and Polar Engineering Conference, pp. 477-481, 2010.
[27] Lade, P.V. & Duncan, J.M., *Cubical Triaxial Tests on Cohesionless Soils*, Journal of The Soil Mechanics and Foundation Division, **99**(10), pp. 793-812, 1973.
[28] Shi, W.C., Zhu, J.G., Chiu, C. F. & Liu, H.L., *Strength and Deformation Behaviour of Coarse-grained Soils by True Triaxial Test*, J. Cent. South Univ. Technol., **17**(5), pp. 1095-1102, October 2010.
[29] Hardin, B.O., *The Nature of Stress Stain Behavior of Soils*, Proceedings of the ASCE Geotechnical Engineering Division Specialty Conference, pp. 3-90, 1978.
[30] Hardin, B.O. & Drnevich, V.P., *Shear Modulus and Damping in soils: Measurement and Parameter Effects (Terzaghi Lecture)*, Journal of the Soil Mechanics and Foundations Division, **98**(6), pp. 603-624, 1972.
[31] Oztoprak, S. & Bolton, M.D., *Stiffness of Sands Through a Laboratory Test Database*, Geotechnique, **63**(1), pp. 57-74, 2013.
[32] Ng, T.T., *Effect of Stress Path on A Two-Size Ellipsoidal Specimen*, 16th ASCE Engineering Mechanics Conference, University of Washington, Seattle, 2003.
[33] Wang, J., *The Stress-Strain and Strength Characteristics of Portaway Sand*. PhD thesis, University of Nottingham, 2005.